

DUAL FREQUENCY CIRCULARLY POLARIZED MICROSTRIP ANTENNA ARRAY

Sergiy Y. Martynuk, Dmytro O. Vasylenko

National Technical University of Ukraine "KPI", Kyiv, Ukraine

Paper contains the most valuable results of experimental and theoretical investigations of dual frequency circularly polarized microstrip antenna array for smart antenna applications with adaptive space-time processing capability. Geometry of the proposed antenna array was optimized for the operation in two frequency bands located inside IEEE *L* band. Presented array structure is composed from ten microstrip radiators independently excited via separate coaxial input ports. Two central radiating elements for two frequency bands have circular shapes with slits and are stacked to provide compact sizes and convergence of their phase centers. Peripheral radiators have annular ring with slits topology. Their geometric centers are superposed with the corners of virtual quadrats with the sides equal to the half of the wavelength for the appropriate band to eliminate the appearance of grating lobes and additional nulls in equivalent radiation patterns. The main feature of the array is its compact packaging that causes significant levels of electromagnetic mutual coupling. Last influences and noticeably deteriorates the shapes of radiation patterns, purity of polarization characteristics and reflection characteristics of planar radiators. The geometric parameters of presented array were selected via multi parametric particle swarm optimization method to provide optimum performance of each radiator in compact array packaging. Moreover, several circularly polarized radiators of the described array assembly were rotated around their centers to improve their characteristics and to increase the quality and effectiveness of latter space-time processing of adaptive antenna system. Novel design of the dual frequency circularly polarized array and imperfection of obtained characteristics are experimentally validated.

Introduction

The application of adaptive antenna (or smart antenna) technology can radically increase the signal-to-noise ratio in great variety of telecommunication systems, radars and navigation complexes. The most typical cases are distinguished when the sources of informational and jamming signals are principally mobile or their angular locations in space are unknown in advance. The good signal-to-noise ratio can be achieved by adaptive tune of the values of weighting coefficients for each array element. The kernel of adaptation procedure is rapid space time processing algorithms applied to the sampled in time complex signals received by radiators separated in space. These algorithms are potentially able to filter the signals coming from the directions of interference sources and simultaneously to amplify the useful ones, incoming from informational sources [1].

Various adaptive algorithms [2], like least mean square or maximum likelihood approaches that explore different criteria and priori conditions, were developed for smart antennas starting from the times of publication of the pioneer work [3]. However, the practical realization of smart antennas is usually associated with a great number of technological and economic constraints. To increase the number of independent array radiators or the absolute value of operating frequency

bandwidth, the required number of synchronized analog transmitting/receiving modules and data rates of analog-to-digital converters as well as the clock frequency of digital signal processors and minimal allocated memory volume are being proportionally increased. As a result, the system becomes prohibitively expensive, not enough reliable or unrealizable at all. Thus, up to day, only relatively small sized smart antenna arrays with several dozens of independent radiators and with operating frequency bandwidth limited to 30–40 MHz were designed [4, 5]. It should be noticed that successful realization and good enough overall performance of even relatively small-sized and narrowband systems can suffer from many other factors caused by not ideal properties of smart antenna elements as well as non-identity of its channels. One should consider the non-identity of electromagnetic characteristics of radiators in small sized array environment, not equal gain factors of analog transmitting/receiving modules, presence of jitters, limited capacity of analog-to-digital converters, limited sequence length of digitized signals etc.

Presented paper discusses the electromagnetic problem of antenna array design following strong requirements of efficient smart antenna realization. Here, the radiation characteristics for the relatively difficult case distinguished by applying the compact dual frequency planar circularly polarized array consisting of ten radiators with separate feed are investigated and optimized.

Formulation of the problem

The up-to-date theory of space-time processing in smart antennas is established on assumption that all components of smart antenna including a radiating part are considered as ideal. It means that identical radiators in smart arrays are assumed to have the same perfect electromagnetic parameters. In major cases, the radiators are considered to be lossless, not coupled and also characterized by purely isotropic radiation patterns. When the plane wave is incident on the array panel from the arbitrary direction (θ, φ) in the upper hemisphere, it induces the same wave by the absolute value portions of signal at array outputs. It is important that signals induced at the array outputs have different phases in frequency domain or time delays in time domain.

For example, consider the planar ($z=0$) array consisting of identical ideal radiators arranged along the regular rectangular grid with element spacing (d_x, d_y) . Eliminating free space attenuation, the traditional signal model that mathematically defines the complex signal $X_{ik}(t)$ received by radiators of smart antenna array can be described by the following relation:

$$X_{ik}(t) = S(t) \exp(j\omega_0 t) \exp(-j\omega \tau_{ik}), \quad (1)$$

where i, k are indexes denoting numbers of corresponding radiators disposed along OX and OY coordinate axes, respectively; $S(t)$ is the complex analytical source signal of the plane wave with the central frequency ω_0 incident from angular direction (θ, φ) ; τ_{ik} denotes the time delay of the signal excited by the plane wave in the radiator with indexes (i, k) . This time delay of the signal can be defined as

$$\tau_{ik} = [(i-1)d_x \sin \theta \cos \varphi + (k-1)d_y \sin \theta \sin \varphi] / c,$$

where c is the velocity of electromagnetic wave in free space.

The idea of simplified theoretical approach (1) implementation is based on the assumption that all radiators receive signals with the same amplitude irrespective to the plane wave direction incidence and its polarization. Thus, each radiator can take the identical part in signal processing that is later reduced to narrowband or broadband digital filtering.

Obviously, the definition (1) is an approximate relation because it does not include electromagnetic behavior of the array composed from realistic radiating elements. Due to the inevitable presence of mutual coupling and mismatch effects, the signals excited by the plane wave on the array radiator outputs are sufficiently different not only in phase component but also in their absolute values.

To correctly describe directional, phase and polarization properties of entire array in its particular environment, it is necessary to use vector and complex definition of the normalized radiation pattern $\mathbf{F}_{ik}(\theta, \varphi)$ of each radiating element, as well as to take into account its realistic properties by introducing the gain factors G_{ik} of each array radiator in relation (1). Then, formula (1) extends to:

$$\mathbf{X}_{ik}(t) = S(t) \mathbf{F}_{ik}(\theta, \varphi) G_{ik} \exp(j\omega_0 t) \exp(-j\omega \tau_{ik}). \quad (2)$$

To eliminate grating lobes and nulls in radiation pattern of the array, the distance between radiators in array should be limited to the half of the wavelength. Consequently, the electromagnetic mutual coupling between radiators principally cannot vanish. In small and average arrays, the absolute majority of radiators are characterized by significantly different amplitude radiation patterns, gain factors and polarization characteristics despite the radiation patterns of each single radiator are unique in the sense of non-uniformity in azimuth planes, inclination of their main lobe directions and polarization purity of radiation characteristics in wide angular sector. These problems become more visible when distances between radiators decrease. Last features very often appear in dual-band or multi-band arrays for navigational, telecommunication, space and airborne adaptive antenna applications where compact array packaging is of great concern. In this context, extremely difficult task is to provide simultaneously azimuthally uniform radiation patterns together with good polarization characteristics over wide angular sector for each radiator.

The deterioration of radiation patterns of array radiators can be partly compensated by setting appropriate values of weighted coefficients during signal processing [6]. To provide the qualitative performance of smart antenna, it is necessary to optimize characteristics of each radiator in array environment.

The purpose of this paper is to present the results of numerical optimization and experimental investigations of dual frequency band circularly polarized planar antenna array applied to solving the problem of space-time processing. During the main electromagnetic problem solution, it is expected to achieve the gain factors for each array radiator to be as high as possible and simultaneously uniform in azimuthal plane, as well as to meet polarization requirements together with low scattering mutual coupling coefficients over operating frequency bands.

According to practical GPS/GLONASS/Galileo navigational tasks, the array with separation between two operating frequency bands 1.3:1 was selected to be in-

vestigated. Presented array structure is manufactured using microstrip antenna technology and composed from 10 independent radiators. The main problem of the developed project was to synthesize the array design with electromagnetic parameters approaching as close as possible to ideal ones.

Application of smart antennas to solving crucial navigational tasks

The navigation signals received from about 20,000 km distant satellites appear to be at least 40 dB below the levels of thermal noises and thus spread spectrum signal processing technique is used to extract the navigation information. Moreover, weak navigation signals from satellite can be masked on certain territory by appropriately designed low power active jammers. Detailed navigation link budget analysis proves that local blocking of navigation equipment can be provided by active jammers having average radiated power around several Watts. In a warfare cases, this means that low cost jammers can introduce inevitably big errors in navigation or absolutely prevent the work of traditional navigation equipment of fighters, cruise missiles, helicopters, tanks, unmanned planes and ships along the territories of dozens square kilometers and thus do not allow them to perform their tasks.

The most efficient suppressing the jamming signals down to the levels of thermal noises can be achieved by the use of board smart antenna arrays with digital beam forming capabilities [7] that are able to create deep nulls of radiation patterns in the directions of jamming or multipath sources via adaptive space-time processing.

GPS (USA) and GLONASS (Russia) are in fact two dominating and conquering systems that provide navigational coverage all over the Earth. Most high responsible navigational complexes use either one or both coverage systems. These two systems have much common properties and sufficient differences regarding the use of operating frequency bands. They utilize closely located in the spectrum frequency bands: GPS *L1* from 1570 to 1585 MHz; GPS *L2* from 1226 to 1237 MHz; GLONASS *L1* from 1593 to 1608 MHz; GLONASS *L2* from 1237 to 1254 MHz. Notation of the frequency bands *L1* and *L2* are accepted by the specialists and are naturally saved in the paper for the band description. The band *L1* is used for civil applications. Operation in *L2* band provides the navigation real time accuracy better than in the case *L1* application (up to 1 m) and can be used for special and military employments. It is clear that complete safety of life smart antenna system for crucial navigational tasks should be capable of processing both GPS and GLONASS signals.

Dual-band antenna array concept

The realization complexity of scanning dual band planar microstrip array is normally caused by the lack of the place on the substrate surface due to overall compact array packaging. Mutual coupling between radiators in dual band array can be reduced by decreasing sizes of each radiator to increase the distance between their metal edges. The implementation of substrates with higher dielectric constant is successful decision of this important problem. It is, however, well known that the radiator size reduction inevitably leads to the frequency bandwidth limitation.

It should be noted, that the radiating planar panel for smart antenna applications principally has separate microwave outputs for each radiator so there is no need in the complicated feeding networks for both bands. From this point of view, its practical realization is easier comparing to the traditional dual band antenna arrays of passive type with single input/output having corporate or series feeding networks for each of two bands. From the other side, traditional passive arrays have no strict requirements on the purity, uniformity and identity of radiation characteristics of separate radiating element in array environment. Common requirement for described types of arrays is the necessity to provide low levels of reflections from the input ports. From the system point of view, the ideology of smart antennas is similar to that of the active antenna arrays, where mutual coupling effects are of great concern because they lead not only to the changing of active reflection coefficient but also to the deterioration of radiation patterns of each radiator.

Relatively low general reliability of smart antennas is limited by the reliability of its electronics such as particularly analog and high speed digital circuits. Most efforts of researchers are directed on increase the lifecycle of smart antennas and decrease their cost. To elongate the lifecycle of small sized smart antennas in practice, it is necessary to develop reconfigurable or switched adaptive systems that use single radiator configuration with traditional receiver when there are no strong sources of interferers. Antenna becomes smart and digital processing blocks turn on within small periods of time when the interfering sources are appearing and beam-scanning with adaptive nulling of radiation pattern is crucially needed.

One of the possible ways to provide this feature is the manufacturing of the separate conventional radiator or traditional array of passive type nearby that radiators used for the adaptive beam-forming. For navigational and some other practically important applications, the single separate radiator can be successfully used but it should be dual band and circularly polarized with phase

center located in the center of small sized smart array panel. This concept was applied to the processing of navigational signals GPS/GLONASS in the severe jamming environment.

Following the described concept, the smart part of the dual band antenna array should contain eight planar radiators. Four radiators should be used in the lower band with the central frequency 1237 MHz and four others in the upper band with the central frequency 1594 MHz. Four radiators ensure a minimum size of smart antenna array which can realize adaptive nulling in the upper hemisphere. They should be disposed in the corners of virtual quadrat with the side equal to half of a wavelength to eliminate grating lobes in the radiation patterns and to provide effective adaptive nulling directed to the jamming source in the upper hemisphere. Smart part of the array is completed by two separate radiators with right circular polarization for each band. Desired accurate solution of navigational task can be achieved in the case of alignment of smart part phase centers of the antenna array and standalone radiators in each band.

The electromagnetic and design problems appeared are complicated in the following aspects. Low loss dielectric substrate type suitable for the creation of array panel under constraints of high efficiency, reliability and compact packaging should be selected. Moreover, right circularly polarized radiators for two bands of the antenna system smart part should be designed as compact as possible. Also, the arrangement of center radiator with compact configuration and separate inputs for two operating bands is required. The configuration of 10 radiators integrated on the surface of common dielectric substrate is proposed. Further optimization of their characteristics in array environment is required to achieve the entire radiating structure performance as good as possible. Each task can be solved in a variety of ways. However, the resultant design can be found as a solution of the compromise problem between contradictory requirements of electromagnetic, systemic, constructional and economical features.

As a dielectric substrate, we use two Rogers TMM 6 Cu folded plates [8] that are ceramic thermoset polymer composite with exceptionally low thermal coefficient of dielectric constant (typically less than 30 ppm/°C) and high reliability of through holes. These TMM 6 substrates are characterized by dielectric permittivity $\epsilon = 6$, loss factor $\tan \delta = 0.0023$ and have different thicknesses $h_1 = 6.3$ mm, $h_2 = 3.175$ mm.

It should be noted that the substrates with lower values of dielectric constant are not applicable here, while compact packaging for dual band array is required. Ac-

ording to our comparative analysis another types of commercially available low loss Cu folded substrates with higher values of $\epsilon > 6$ are at least twice more expensive, technologically less suitable for making via-holes and have worse thermal stability characteristics. In addition, the dielectric constant growth reduces the radiator size and limit maximum operating bandwidth of the radiator. Stacked arrangement of two substrates was proposed to provide the design of central radiating elements for the operation in the case of jamming absence.

In the described design, the thicker TMM 6 substrate with $h_1 = 6.3$ mm is located at the bottom of the stacked sandwich. It performs the function of purely dielectric layer, where the double-sided copper metallization is completely removed. Complicated metal configuration of array is manufactured from the double-sided metallization of thinner TMM 6 substrate that is fixed without air gaps at the top of the stacked design. Both substrates have holes to organize contact type feed of each radiator via coaxial probes. Thinner substrate is technologically metallized whereas the thicker one has no metallization.

The class of circularly polarized microstrip radiators is well studied. These microstrip radiators contain dozens of different shaped and sometimes exotic configurations [9]. To form the circular polarization, all of them utilize similar method based on the simultaneous excitation of two orthogonal and 90° phase shifted microstrip resonator fundamental modes with equal amplitudes. One of the known ways of the circular polarization organization is feeding the symmetrical resonator from the orthogonal sides by two-wave power splitter with 90° additional delay section disposed in one of the output channels.

The circular polarization can be also formed automatically by incorporating slight asymmetry into the microstrip resonator geometry and using single excitation line connected (or electromagnetically coupled) with appropriate feed region. Obviously, the second way is more attractive because the microstrip resonator topology occupies noticeably less space on the surface of the supporting dielectric substrate. The radiating microstrip resonator can be performed as rectangular, elliptical, quadratic or circular shaped geometry having ledges or slits, triangular with slots, annular-ring with slits etc.

Our theoretical investigations show that annular-ring geometry with 45° disposed slits is better suited among others for the considered task solution because it has more compact sizes, slightly lower mutual coupling levels not exceeding 1–2 dB, wider frequency band-

width of circular polarized performance as well as higher freedom in variation of geometry parameters under optimization compared to conventional quadratic or circular designs.

The topology of right circularly polarized annular ring microstrip resonator with 45° arranged slits is schematically shown in Fig. 1. The annular ring having inner radius $R1$ and outer radius $R2$ is printed on the top surface of stacked TMM 6 substrates with thickness values h_1 and h_2 . Orthogonal near-degenerate fundamental modes TM_{11} are excited by pair of 45° oriented slits of $s \times t$ size to provide right circular polarization performance.

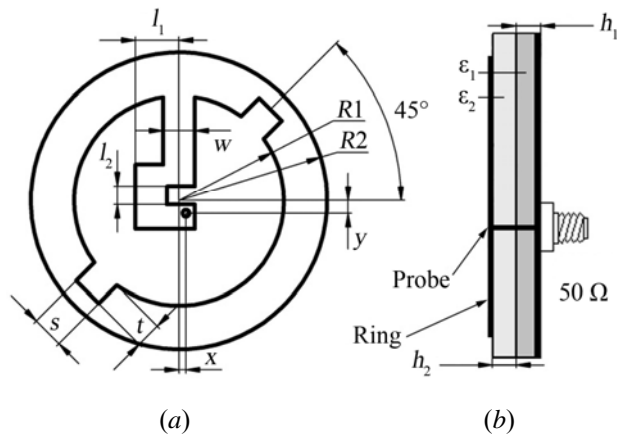


Fig. 1. The topology of circularly polarized microstrip radiator: (a) annular ring with a pair of slits; (b) the side view of composed structure with 50 Ohm coaxial line connector.

Radiating annular resonator is excited by w width curved microstrip line disposed on the inner boundary of annular ring. Coaxial probe feed is connected to the curved microstrip line in its initial point shifted from the ring center by x, y values along two orthogonal axes. The microstrip line having design parameters l_1 and l_2 as well as x, y performs the function of quarter-wavelength transformer. The input impedance matching condition for annular ring radiating resonator in the first approximation can be expressed as follows [10]:

$$Z_T [(Z_A + jZ_T \tan \beta l) / (Z_T + jZ_A \tan \beta l)] = 50 \quad (1)$$

where Z_A denotes input impedance of annular ring from the inner side; Z_T defines the impedance of w width microstrip line; β, l are propagation constant and total length of curved microstrip line. Detailed electromagnetic analysis of annular ring microstrip radiator present in [11] shows that curved configuration of feeding microstrip line as well as slit sizes sufficiently influence the input impedance Z_A .

To obtain good circularly polarized performance, the multiparametric optimization of annular ring microstrip

radiator shown in Fig. 1 was performed by particle swarm optimization method. Calculated parameters of standalone microstrip annular ring radiator for both $L1$ and $L2$ bands are presented in Table 1.

Table 1. Calculated parameters of standalone microstrip annular ring radiator

Parameters of annular ring, mm	L1 band	L2 band
$R1$	12.48	15.04
$R2$	16.07	21.25
x	5.7	1
y	0.31	1.85
w	4.2	4.5
t	1.3	3.67

Two experimental samples of annular ring radiator were manufactured and all-round tested using test facility of Antenna laboratory of NTUU “KPI”. Fig. 2 presents the photo of the test sample of standalone circularly polarized annular-ring antenna optimized for the $L1$ band. The sample was manufactured on stacked TMM 6 substrates with overall thickness $3.175+6.3$ mm and sizes 100×100 mm. Dielectric substrates were fixed by four screws at the corners to massive screen aluminium plane. The obtained construction is fixed in addition which holds to provide perfect contact with input 50 Ohm coaxial structure ended by standard panel type SMA connector.



Fig. 2. Photo of manufactured standalone annular ring radiator designed for operation in the $L1$ band.

Measured and calculated frequency dependencies of input reflection coefficient of manufactured annular-ring radiator shown in Fig. 2 are depicted in Fig. 3. It can be seen that calculated results are in good agreement with experimental data. Slight shift of calculated antenna frequency response relatively to measured one

can be explained by increasing of resonator size due to 20 μm thickness protective plating on the surface of Cu foil. Achieved input impedance frequency bandwidth for the level of $\text{VSWR} < 1.5$ approaches 95 MHz or 5.9%.

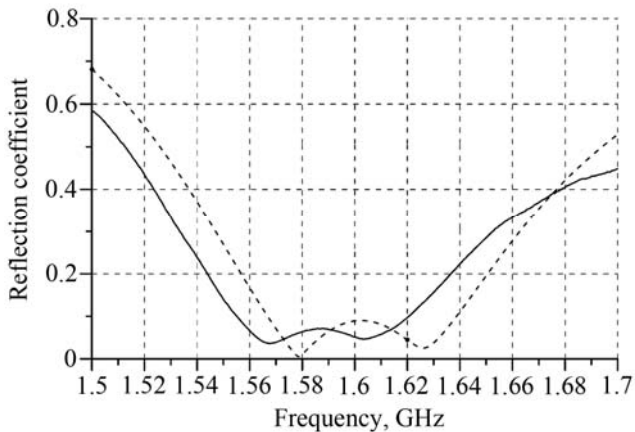


Fig. 3. Calculated (dashed line) and measured (solid line) frequency dependencies of reflection coefficient of radiator shown in Fig. 2.

To measure the circularly polarized radiation characteristics of annular ring antenna with the pair of slits, a precise spiral antenna having axial ratio better than 0.9 along main axis was manufactured and used. Measured radiation patterns in horizontal plane of annular ring antenna shown in Fig. 2 for right circular polarization are presented in Fig. 4 for five frequencies inside the $L1$ band. Presented curves are close to each other but indicate the existence of non-uniformity (non-symmetry) in measured radiation patterns even for the case of stand-alone annular ring antenna. Described non-uniformity of radiation patterns increases with growth of elevation angle.

Similar non-uniformity is observed in the direction closer to the substrate surface planes, where the gain factor of antenna is less than in main direction. These directions are typical for low-elevation navigation satellites which signals are used for the definition of investigated object coordinates. The non-uniformity of experimentally obtained radiation characteristics of the test sample in azimuthal plane can be caused by the finiteness of the screen which sizes are approximately equal to half of the wavelength and by the presence of coaxial cable on its opposite side. This conclusion was proved by similar measurements of the test sample manufactured for the use within frequency band $L2$. It should be noted that the obtained level of non-uniformity of radiation pattern in azimuthal plane does not exceed 3–5 dB. Therefore, this non-uniformity can be considered as acceptable in the case of smart antenna applications because it can be relatively easy compen-

sated in a given direction by using the weighted coefficients during digital signal processing. Moreover, the influence of considered effect can be significantly decreased by the enlargement of the metal screen sizes.

Described above concept of switched dual band circularly polarized smart antenna system assumes the necessity of central radiator that provides the normal performance of the navigational equipment in absence of active jamming interferers. To obtain high positioning accuracy, the central radiating element should provide circularly polarized performance in both $L1$ and $L2$ bands extended to include GPS and GLONASS spectrum component. Although appropriate dual band antenna designs are well known and widely used [12], they are not applicable here because space limitations dictated by peripheral radiators used for adaptive space-time processing. Certainly, it is possible to remove central element from compact array package and to place it somewhere aside. However, this arrangement leads to the overall system dimension increase and introduces unacceptable ambiguity in navigational solution because phase centers of array and removed central radiator occur to be sufficiently separated.

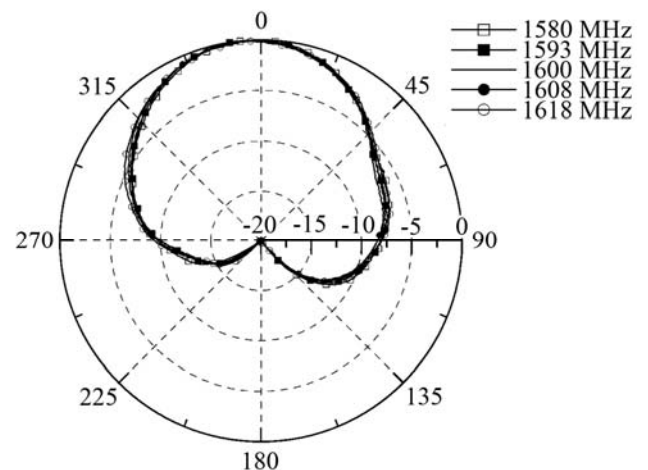


Fig. 4. Measured (in dB) radiation patterns in horizontal plane of annular ring antenna shown in Fig. 2.

Novel design of stacked dual band circularly polarized radiator was proposed and optimized (Fig. 5). To provide the operation in dual band, two stacked circular patch resonators are excited by independent coaxial probe feeds. Both resonators are etched from double sided metallization of the upper TMM 6 substrate with the thickness $h_2 = 3.175$ mm. Low ($R4 = 24.15$ mm) and upper ($R3 = 20.83$ mm) circular patch resonators are placed on bottom and top sides of the substrate respectively. Their topologies additionally contain slits ($a_2 \times b_2$ and $a_1 \times b_1$) and ledges ($c_2 \times d_2$ and $c_1 \times d_1$) in orthogonal planes to provide right circularly polarized

operation within frequency bands $L1$ and $L2$. To minimize mutual coupling between stacked resonators, they are rotated on the angle 90° to each other. Coaxial probe feeds for both resonators are soldered only on the top surface of the TMM 6 substrate that is a distinctive feature of presented dual band design.

Coaxial probe for the excitation of upper patch resonator $R3$ is coming through both substrates and have no contact with resonator $R4$ due to small air gap etched from its surface. Metal contact of probe feed with the $L2$ band resonator printed on the opposite side of the substrate is provided by metallization via connected small metal plate isolated from $L1$ band resonator by air gap. Last technique allows soldering probes only from the top side of the upper substrate of the sandwich. Parameters of both resonators and the positions of coaxial probe feeds $(x_1, y_1; x_2, y_2)$ were optimized using similar software as for the optimization of annular-ring patch radiators.

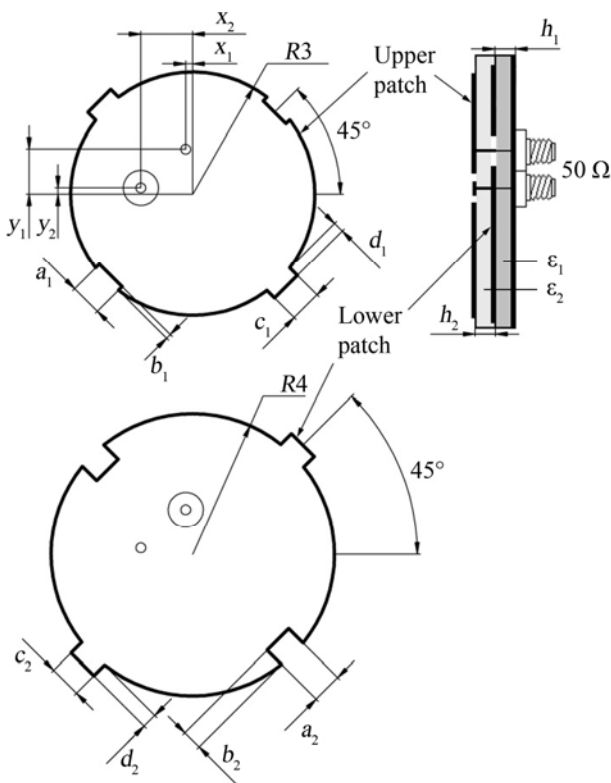


Fig. 5. Stacked circular with slits topology of circularly polarized dual-band central radiator: top and bottom resonators and their side view.

Obvious drawback of the presented design is that the patch resonators utilize thinner substrates $h_2 = 3.175$ mm for $L1$ band and $h_1 = 6.35$ mm for $L2$ band comparing to annular ring, where full stack thickness is $h_1 + h_2 = 9.525$ mm. Calculated and experimental results show that the frequency bandwidth of dual band

antenna is three times less for $L1$ band and 1.5 times less for $L2$ band comparing to annular ring patches described above. Another restriction is strong mutual coupling between stacked closely located resonators. It causes relatively poor level of isolation between input ports that reaches the peak values -7 dB for $L2$ band and -18 dB for $L1$ band.

Presented design was employed to compose complete dual band right circularly polarized radiating panel for the switched smart antenna. Manufactured test sample of the optimized 10-element radiating panel is presented in Fig. 6. The disk made from aluminum with the diameter 260 mm serves as a metal screen constructional basis for two stacked low loss dielectric substrates and transitions from coaxial cables to coaxial probes. The dielectric TMM 6 substrates have thicknesses $h_1 = 6.35$ mm and $h_2 = 3.175$ mm respectively. Bottom substrate of the thickness h_1 has no Cu foil at all. The metal topology of ten microstrip radiators with coaxial probe feed is etched from the double sided Cu metallization of the upper substrate of the thickness h_2 .

Radiating panel of circularly polarized switched smart antenna array is composed from 4 peripheral annular ring radiators for the frequency band $L1$, 4 peripheral annular ring radiators for the frequency band $L2$ and two stacked central circular radiators with slits and ledges disposed on the top for $L1$ band and on the bottom for $L2$ band respectively. Peripheral radiators for both $L1$ and $L2$ bands are arranged at the corners of virtual quadrats with the sides exactly equal to the half of wavelength for each band namely 93.8 mm for $L1$ and 120 mm for $L2$. To provide the coincidence of the phase centers of the 4-element radiating systems, the virtual quadrats are rotated on the angle 45° as shown in Fig. 6.



Fig. 6. Manufactured test sample of 10-element dual band circularly polarized switched smart antenna array. The central element for $L2$ band is hidden.

The design features of the dual frequency central and single frequency peripheral radiators of the circularly polarized array were already shown and described above in detail (see Fig. 1, 5). At the first designing step, geometries of peripheral and central radiators were optimized separately using particle swarm method of multi-parametric optimization. The goal function minimizing the reflection coefficient and providing circularly polarized performance with the axial ratio better than -3 dB in required frequency ranges was selected for the optimization. At the second step of the project, the numerical model of 10-element radiating panel in which radiators with separately optimized geometries were integrated on the common substrate sandwich was developed and investigated. As expected, mutual coupling effects in compact antenna array assembly sufficiently deteriorate the shape and symmetry of radiation patterns and lead to the degradation of reflection and axial ratio characteristics of all radiators.

To decrease the parasitic influence of mutual coupling, some radiators were axially rotated through angles 90° , 180° or 270° . Parameters of all radiators were additionally optimized taking into account compact packaging. Last procedure required time consuming calculations. It was impossible to obtain perfect characteristics of all radiators for all frequencies from required band but their absolute majority were managed to become sufficiently better. As an example, the measured and calculated right circularly polarized radiation patterns for two peripheral radiators operating in $L1$ band are presented in Fig. 7 and Fig. 8.

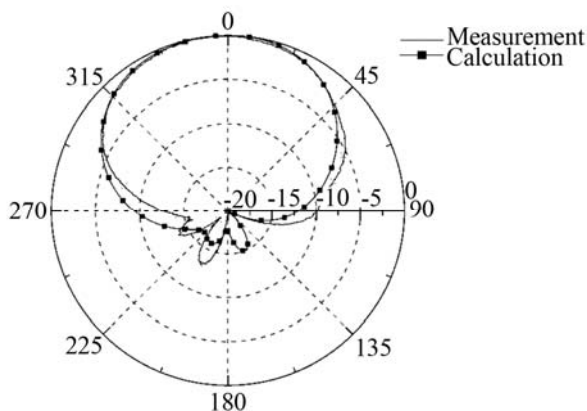


Fig. 7. Radiation patterns of the peripheral radiator optimized for $L1$ band and located at the far end of the array structure as seen in Fig 6.

Fig. 9 contains frequency dependencies of reflection coefficients of peripheral radiator operating within $L1$ band. Fig. 10 shows similar characteristics of two central radiators for both bands. Obviously, reflection coefficients of radiating elements in compact array packag-

ing noticeably differ from each other and the characteristics of standalone radiator shown in Fig. 3.

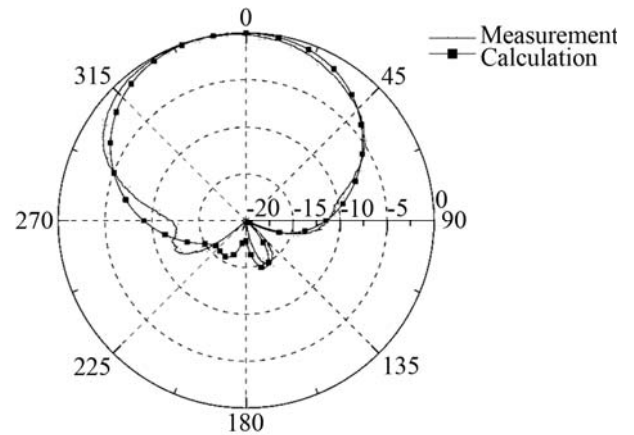


Fig. 8. Radiation patterns of the peripheral radiator optimized for $L1$ band and located at the close end of the array structure as seen in Fig 6.

As seen from Fig. 9, the reflection coefficients do not exceed -13 dB for all peripheral radiators optimized for the operation in $L1$ GPS/GLONASS frequency band. Measured axial ratios in zenith direction are not worse than -3 dB for all radiators. Non-uniformity of their radiation patterns in azimuthal plane for $L1$ and $L2$ peripheral radiators does not exceed ± 3 dB for the elevation angles 15° – 50° and ± 1 dB for the elevation angles 50° – 90° . Their average measured right circularly polarized realized gain values are close to 5 dB in the operating frequency bands. Similar measured characteristics have been obtained for four peripheral radiators of $L2$ GPS/GLONASS frequency band.

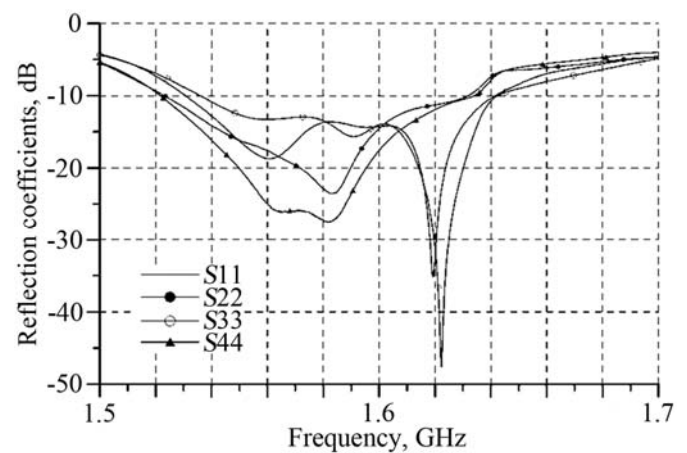


Fig. 9. Reflection coefficients in dB versus frequency for peripheral $L1$ band radiators.

The optimization of the central radiating element seemed to be the most complicated task because its characteristics in each band are greatly influenced by closely located peripheral radiators and by the radiating

part of stacked central radiator of another band. As seen from curves shown in Fig. 10, the reflection versus frequency does not exceed the level -10 dB that is considered to be acceptable for the case when the jamming sources are absent.

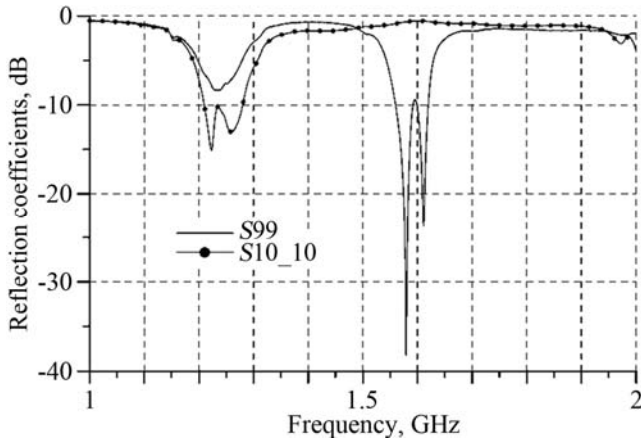


Fig. 10. Reflection coefficients in dB versus frequency for two central stacked radiators designed for operation in $L1$ and $L2$ bands.

Mutual coupling between peripheral radiators after their rotating and multiparametric optimization were minimized down to the levels -13 dB. After optimization, these characteristics become better than those shown in Fig. 11.

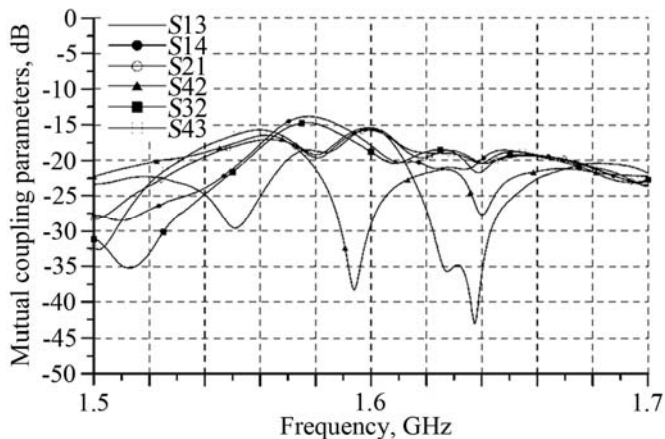


Fig. 11. Mutual coupling parameters versus frequency for $L1$ peripheral radiators matched to $L1$ band.

Conclusion

The novel design of 10-element dual band right circularly polarized radiating panel for switched smart antenna applied for crucial navigational task was introduced. Radiating panel contains 4 peripheral radiators for $L1$, 4 peripheral radiators for $L2$ and two central stacked radiators with independent feeds for $L1$ and $L2$ GPS/GLONASS frequency bands. It was shown that annular ring resonators are well suited as a basic shape

of peripheral radiators that are used for adaptive beamforming. To reach acceptable radiation and reflection characteristics of all radiators in compact array environment, they were axially rotated and their geometry was optimized by particle swarm optimization method taking into account compact array packaging.

Paper contains photos of manufactured test samples of single frequency annular ring radiator, dual frequency stacked radiator and optimized dual frequency array structure composed from them. Presented measured data and theoretical results show good agreement.

Acknowledgment

The authors would like to express great thanks to the staff of NAVIS Ukraine Ltd for encourage, financial support of the project and manufacturing the array structure test samples. The authors would like to thank Anatoliy G. Laush, principal and general engineer of NAVIS Ukraine for his active participation in the project and kind support.

References

1. Mukhopadhyay M., Sarkar B. K., Chakraborty A. Augmentation of anti-jam GPS system using smart antenna with a simple DOA estimation algorithm // *Progress in Electromagnetics Research*. — 2007. — Vol. 67. — P. 231–249.
2. Smart antennas — state of the art. Eurasip series / T. Kaiser, A. Bourdoux, et al. — New York: Hindawi Corporation, 2009. — 864 p.
3. Adaptive antenna systems / B. Widrow, P. E. Mantey, L. J. Griffiths, B. B. Goode // *IEEE Proceedings*. — 1967. — Vol. 55, N. 12. — P. 2143–2159.
4. Brown A. High accuracy GPS performance using digital adaptive beamforming technique // *Proceedings of ION National Technical Meeting, Long Beach, January 2011*. — P. 210–218.
5. Smart antenna terminals for broadband mobile satellite communications at Ka-band / A. Geise, A. Jacob, K. Kuhlmann, H. Pawlak, et al. // *Proceedings of International ITG Conference on Antennas, Munich, Germany, April 2007*. — P. 57–60.
6. Huang Z., Balanis C. A., Birtcher C. R. Mutual coupling compensation in UCAs: Simulations and experiment // *IEEE Transactions on Antennas and Propagation*. — 2007. — Vol. 54, N. 11. — P. 3082–3086.
7. GALANT — Galileo antenna demonstrator for safety critical applications / M. Cuntz, A. Konovaltsev, A. Hornbostel, et al. // *Proceedings of European Conference on Antennas and Propagation, Berlin, Germany, 2010*. — P. 1103–1105.
8. Rogers Corporation, USA — www.rogerscorporation.com.
9. Wong K. L. Compact and broadband microstrip antennas. — New York: John Wiley & Sons, 2002. — 300 p.
10. Chen H. M., Wong K. L. On circular polarization design of annular-ring microstrip antennas // *IEEE Transactions on Antennas and Propagation*. — 1999. — Vol. 47, N. 8. — P. 1289–1292.
11. CST Microwave Studio. — Manual, 2008.

Received in final form October 16, 2011